IEEE Access
Multidisciplinary ⋮ Rapid Review ⋮ Open Access Journal

Received 18 March 2024, accepted 9 May 2024, date of publication 21 May 2024, date of current version 30 May 2024.
Digital Object Identifier 10.1109/ACCESS.2024.3403892

RESEARCH ARTICLE

Maximum Likelihood Estimators of Generalized Gaussian Distribution With an $\mathbb{H}$-Proper Quaternion Random Variable

ROBERT KRUPIŃSKI[1,2], TOMASZ MARCINIAK[1], AND OLUTAYO O. OYERINDE[1,3], (Senior Member, IEEE)
[1]Faculty of Telecommunications, Computer Science and Electrical Engineering, Bydgoszcz University of Science and Technology, 85-796 Bydgoszcz, Poland
[2]Department of Signal Processing and Multimedia Engineering, West Pomeranian University of Technology in Szczecin, 71-126 Szczecin, Poland
[3]School of Electrical and Information Engineering, University of the Witwatersrand at Johannesburg, Johannesburg 2050, South Africa
Corresponding author: Robert Krupiński (rkrupinski@zut.edu.pl)

ABSTRACT The currently known generalized Gaussian distributions (GGD) with an augmented quaternion random variable are based on the 3D GGD distribution. That is, they are based on random variables with three components. In this article, GGD for an augmented quaternion random variable based on GGD for a random variable with four components is given. Then the distribution obtained is simplified for an $\mathbb{H}$-proper quaternion random variable. For this simplified distribution the maximum likelihood estimators are presented. The simplification allows the presentation of the ML estimator for the shape parameter of GGD by eliminating the coefficients related to the covariance from the non-linear equation. The performance of the derived ML estimators is examined in the simulations.

INDEX TERMS Augmented quaternion statistics, maximum likelihood method, quaternion generalized Gaussian distribution, quaternion random variable.

I. INTRODUCTION

Signal processing using statistical methods enjoys unflagging interest. Therefore, new tools for determining the parameters of the observed processes are being designed, and new techniques for generating processes for given model parameters are being created. Statistical signal processing is used in more and more research areas. The generalized Gaussian distribution (GGD), among other things, is of such interest to scientists. GGD has been widely used in various engineering applications. GGD itself has been extended to various types of random variables, as well as to multivariate random variables. Thus, different types of signals and processes can be modeled with GGD. Many methods of determining the parameters of this distribution have been developed too.

This distribution can be found under other names in the literature:

The associate editor coordinating the review of this manuscript and approving it for publication was Diego Bellan.

- GND – the generalized normal distribution,
- the Subbotin distribution,
- GED – the generalized error distribution,
- EPD – the exponential power distribution (also called as the Box-Tiao distribution [1]).

The generalized Gaussian probability density function for a continuous random variable is [2] and [3]

$$f(x) = \frac{\lambda \cdot p}{2 \cdot \Gamma\left(\frac{1}{p}\right)} e^{-[\lambda \cdot |x|]^p}, \tag{1}$$

where $\Gamma(\cdot)$ is the gamma function $\Gamma(z) = \int_0^\infty t^{z-1} e^{-t} dt$, $z > 0$ [4], p is the shape parameter and λ depends on p and the standard deviation of the distribution [5].

This distribution owes its popularity to the inclusion of various other distributions, from super–Gaussian, Gaussian to sub–Gaussian. Depending on the p value of the shape parameter, special cases of GGD are obtained, which are known distributions:

- $p = 1$: the Laplacian distribution (LD), (also called the double exponential distribution),
- $p = 2$: the Gaussian distribution (GD),
- $p \to \infty$: a uniform distribution,
- $p \to 0$: an impulse function,
- $p = 1/2$: introduced in [6],
- $p = 1/3$: presented in [7],
- $p = 1/m$ for $m = 2, 3, \ldots$: covered in [8].

Based on special cases, the analysis and calculations can be simplified and equations can be determined in closed form.

The most popular method for determining distribution parameters is the maximum likelihood (ML) method. The ML method for determining the shape parameter p of the one-dimensional GGD distribution described by formula (1) was given by Du [3]

$$\frac{\Psi(1+\frac{1}{\hat{p}})+\log(\hat{p})}{\hat{p}^2}+\frac{1}{\hat{p}^2}\log\left(\frac{1}{N}\sum_{i=1}^{N}|x_i|^{\hat{p}}\right)-\frac{\sum_{i=1}^{N}|x_i|^{\hat{p}}\log(|x_i|)}{\hat{p}\sum_{i=1}^{N}|x_i|^{\hat{p}}}=0, \tag{2}$$

where N denotes the number of observed variables, and $\{x_1, x_2, \ldots, x_N\}$ is the collection of N i.i.d. zero-mean random variables and where

$$\Psi(\tau) = -\gamma + \int_0^1 (1-t^{\tau-1})(1-t)^{-1}dt, \tag{3}$$

and $\gamma = 0.577\ldots$ denotes the Euler constant. Equation (2) must be solved numerically due to $\hat{p}$. The λ parameter is also determined by the ML method for the known shape parameter p found in the previous equation (2)

$$\lambda = \left(\frac{N}{p\cdot\sum_{i=1}^{N}|x_i|^p}\right)^{\frac{1}{p}}. \tag{4}$$

Many articles have been published presenting the applications of GGD in many research areas, e.g., in image segmentation [9], stereoscopic images [10], image synthesis [11], the binarization of historical degraded document images [12], image compression [7], [13], [14], in testing adaptive filters [15], and the vibroacoustic method of detecting damage to the power transformer core [16]. In [17] the probabilistic function as a mixture of generalized Gaussian distributions was built in order to predict the failure of rotating machines. Thus, the generalized Gaussian hidden Markov model (GGHMM) was created for machinery prognostic purposes. A new statistical image watermarking scheme in nonsubsampled Shearlet transform (NSST) domain was proposed by Wang et al. [18]. It was based on the bounded generalized Gaussian mixture model (BGGMM) based hidden Markov tree (HMT). Whereas, BGGMM was introduced in the paper [19]. Discrete wavelet coefficients were modeled using GGD in image watermarking techniques [20], texture retrieval [21], [22], fingerprint image compression [23], image denoising [24], and texture classification [25]. Allili [26] proposed a new statistical framework based on finite mixtures of generalized Gaussian (MoGG) distributions to represent the marginal distribution of the wavelet coefficients and described its application to texture discrimination and retrieval. Multiresolution image denoising schemes in the wavelet domain were analyzed in [27]. GGD has been used in a variety of other applications, in probabilistic classifiers [28], in an automatic change detection in multitemporal SAR images [29]. GGD for modeling multiple access interference in ultra-wide bandwidth (UWB) systems was applied in [30].

The Gaussian, the generalized Gaussian and all the compound Gaussian distributions are encompassed by the elliptically symmetric (ES) distributions [31]. An extension of the matrix Slepian–Bangs (SB) formula to ES distributions was considered and the closed-form expression of a simple corrective coefficient for GGD was given in [31].

GGD is also a special case of the generalized Gamma distribution (GΓD) [22]. These two distributions were compared by Song [32].

The complex generalized Gaussian distribution (CGGD) was extensively discussed in [33]. The paper presented a procedure for generating complex random variables for this distribution. The shape and covariance parameters in the complex domain were estimated by a maximum likelihood estimation (MLE) method. And finally, CGGD was applied to actual radar data. Testing the circularity of CGGD can be found in [34].

CGGD belongs to the wide family of complex elliptically symmetric (CES) distributions [35], [36], [37]. The Fisher information matrix (FIM) for the estimation of the shape and scale parameters, and the normalized covariance matrix, also called scatter matrix, for CGGD were derived in [35]. CGGD was applied in a wide variety of signal processing applications, e.g., in medical imaging [38]. A detector based on convolutional neural networks (CNNs) for spectrum sensing (SS) problems under various noise models (among others, isometric CGGD) was considered in [39].

In order to model multidimensional signals, the multivariate generalized Gaussian distribution (MGGD) was used (also called the multivariate power–exponential distribution [40], [41]). The maximum likelihood method for estimating the parameters of MGGD was addressed in [42], whereas a Riemannian averaged Fixed-Point algorithm was introduced in [43].

In [44] an unsupervised classifier based on a finite mixture model using the multivariate generalized Gaussian distribution was introduced. This classifier was applied on a dataset of weld defect radiographic images. In order to achieve timely and accurate detection of downhole faults, a systematic fault detection method was proposed based on MGGD and the Kullback Leibler Divergence (KLD) [45], [46].

The beginning of quaternions is attributed to Hamilton [47]. Quaternions are a noncommutative extension of complex numbers [48]. Quaternions allow you to model signals in three– and four–dimensional space. $\mathbb{H}$ denotes the algebra of quaternions. The concept of $\mathbb{H}$-properness was introduced in [49] as the invariance of the probability density function (pdf) of a quaternion–valued variable q under an arbitrary axis and angle of rotation ϕ — a variable q is said to be proper, if $pdf(q) = pdf(e^{\eta\phi}q)$ for any pure unit quaternion η. Random variables and processes with a vanishing pseudo–covariance are called proper [50], [51]. Properness in the quaternion domain, also denoted as $\mathbb{H}$-properness, is based on the vanishing of three different complementary covariance matrices [51].

Took et al. [52] discussed extensively the augmented quaternion statistics. Augmented quaternion second–order statistics have been used in several applications, among others:

- the nonlinear minimum mean–squared error (MMSE) estimation problem [53],
- the independent component analysis (ICA) [54],
- the quaternion–valued echo state networks (QESNs) for nonlinear adaptive filtering [55],
- the quaternion widely linear (QWL) processing [51], [52], [56], [57],
- the widely linear quaternion-valued Kalman filter (WL–QKF) and widely linear quaternion-extended Kalman filter (WL–QEKF) [58],
- the adaptive widely linear quaternion least mean square (WL–QLMS) algorithm for the modeling and forecasting of three dimensional wind field [59],
- the widely linear quaternion multiple-model adaptive estimation (WL–QMMAE) algorithm based on the widely linear quaternion Kalman filter and Bayesian inference [60],
- the augmented quaternion extreme learning machine (QELM) models for quaternion signal processing [61],
- and the augmented online sequential quaternion extreme learning machine (OS–QELM) for the real-time learning of feedforward neural networks [62].

A variational autoencoder (QVAE) in the quaternion domain $\mathbb{H}$ leveraging the augmented second–order statistics of $\mathbb{H}$-proper signals was analyzed in [63]. Augmented quaternions were used for remaining useful life (RUL) estimation of rolling bearings [64], for degradation prognostics of rolling bearings [65]. A generic reproducing kernel Hilbert space (RKHS) framework for the statistical analysis of augmented quaternion random vectors was presented in [66].

Real-world seismic signals cannot be completely described using existing Gaussian models [67], hence the generalized Gaussian distribution with an augmented quaternion variable (QGGD) was used in [68]. QGGD parameterized variations in the vector–quaternion during the presence and absence of a polarized source (human footsteps) were presented. The data from the three orthogonal channels was treated as a pure quaternion. In order to quantify the inter–channel correlation of the tri–axial geophone, the augmented covariance matrix of QGGD was used. In the absence of footsteps, random Gaussian noise with comparable power in all the three channels of the geophone was observed. Since there exists no correlation between the orthogonal axes, an unpolarized $\mathbb{Q}$-proper diagonal structure was obtained. Footstep signals were expected to be $\mathbb{Q}$-improper due to the presence of elliptically polarized signals. Venkatraman et al. [68] iteratively looked at values in the $< 0.1, 2 >$ range to estimate the shape parameter as the best chi-square fit.

The 3D generalized Gaussian distribution (3D GGD) parameterized by the shape parameter p and the covariance matrix C was revised in [69]. Based on that, the alternative QGGD was derived for an augmented quaternion valued random variable. The procedure for generating the augmented quaternion valued random variables was defined for this distribution. In the case of pure quaternions, this probability density function becomes a limiting case. Therefore, for this case, the dedicated generalized Gaussian distribution of an augmented quaternion random variable for pure quaternions was introduced in [70].

As it has been shown, GGD is widely used and various variants of GGD appear in the literature. It has also been shown that augmented quaternions are used in many research areas. Therefore, there is a need to model processes using new models. Accordingly, a new GGD will be given in the article.

The article presents 4D GGD with a random variable consisting of four components. This is to correspond to the four components of a full quaternion. 4D GGD is the basis for creating GGD with an augmented full quaternion random variable. In previous works, GGD with an augmented quaternion random variable was based on 3D GGD.

The rest of the paper is organized as follows. In Section II-A, augmented quaternion statistics is recalled. Then, Section II-B describes MGGD. 3D GGD and QGGD are presented in Section II-C. Then, 4D GGD based on MGGD for a full quaternion from Section III is extended for an augmented quaternion random variable in Section IV and then simplified for an $\mathbb{H}$-proper quaternion random variable in Section V. Section V-A describes the ML equations for GGD with an $\mathbb{H}$-proper quaternion random variable. Section VI presents numerical experiments to show the performance of the ML estimators.

II. DEFINITIONS

A. AUGMENTED QUATERNION STATISTICS

Augmented quaternion statistics is recalled on the basis of the articles [52], [69], [70] and will be used in later sections.

A full quaternion can be represented by real numbers q_a, q_b, q_c, and q_d and three axes $\imath$, $\jmath$, κ as: $q = q_a + \imath q_b + \jmath q_c + \kappa q_d$. A full quaternion $q = q_a + q_p$ consists of a real part q_a and a vector part $q_p = \imath q_b + \jmath q_c + \kappa q_d$ (also called a pure quaternion or a vector quaternion).

The orthogonal unit vectors $\imath$, $\jmath$, $and \kappa$ satisfy the following relations [52], [69]

$$\imath\jmath = \kappa \qquad \jmath\kappa = \imath \qquad \kappa\imath = \jmath,$$

$$\imath\jmath\kappa = \imath^2 = \jmath^2 = \kappa^2 = -1. \tag{5}$$

Quaternions can be represented in vector form: a full quaternion as a real valued quadrivariate vector $\overrightarrow{q} = [q_a, q_b, q_c, q_d]^T$ and a pure quaternion as a real valued trivariate vector $\overrightarrow{q_p} = [q_b, q_c, q_d]^T$.

The augmented quaternion can be represented in vector form [49], [52]: $\overrightarrow{q^a} = [q, q^\imath, q^\jmath, q^\kappa]^T$, where three perpendicular quaternion involutions (self-inverse mappings) are given by [52] and [69]

$$\begin{aligned} q^\imath &= -\imath q \imath = q_a + \imath q_b - \jmath q_c - \kappa q_d, \\ q^\jmath &= -\jmath q \jmath = q_a - \imath q_b + \jmath q_c - \kappa q_d, \\ q^\kappa &= -\kappa q \kappa = q_a - \imath q_b - \jmath q_c + \kappa q_d. \end{aligned} \tag{6}$$

The dependence of the augmented quaternion on a real valued quadrivariate vector can be represented by a transformation [52], [69]

$$\begin{bmatrix} q \\ q^\imath \\ q^\jmath \\ q^\kappa \end{bmatrix} = \begin{bmatrix} 1 & \imath & \jmath & \kappa \\ 1 & \imath & -\jmath & -\kappa \\ 1 & -\imath & \jmath & -\kappa \\ 1 & -\imath & -\jmath & \kappa \end{bmatrix} \begin{bmatrix} q_a \\ q_b \\ q_c \\ q_d \end{bmatrix}, \tag{7}$$

and in abbreviated form

$$\overrightarrow{q^a} = A \cdot \overrightarrow{q}. \tag{8}$$

The inverse of the matrix A is [52] and [69]

$$A^{-1} = \frac{1}{4} A^H, \tag{9}$$

where $(\cdot)^H$ denotes a quaternion conjugate transpose operator. Given the equation (9), the quaternion conjugate transpose of the inverse matrix A^{-1} is

$$A^{-H} = \left(A^{-1}\right)^H = \left(\frac{1}{4} A^H\right)^H = \frac{1}{4} A. \tag{10}$$

The inverse of the transformation (8) where a real valued quadrivariate vector depends on an augmented quaternion can be represented by [52] and [69]

$$\overrightarrow{q} = \frac{1}{4} A^H \cdot \overrightarrow{q^a}. \tag{11}$$

The determinant of A is [52]

$$|A| = 16. \tag{12}$$

It can be found from the LU decomposition and the product of its diagonal entries or as a product of its singular values.

For a full quaternion as a random variable of the form $\overrightarrow{Q} = [Q_a, Q_b, Q_c, Q_d]^T$, the covariance matrix C can be determined as the expected value $E\{\cdot\}$ of the product $\overrightarrow{Q} \cdot \overrightarrow{Q}^T$. The real valued quadrivariate covariance matrix C is then [69]

$$\begin{aligned} C &= E\{\overrightarrow{Q} \cdot \overrightarrow{Q}^T\} = E\{\overrightarrow{Q} \cdot \overrightarrow{Q}^H\} \\ &= \begin{bmatrix} \sigma^2_{Q_a} & \sigma_{Q_a Q_b} & \sigma_{Q_a Q_c} & \sigma_{Q_a Q_d} \\ \sigma_{Q_b Q_a} & \sigma^2_{Q_b} & \sigma_{Q_b Q_c} & \sigma_{Q_b Q_d} \\ \sigma_{Q_c Q_a} & \sigma_{Q_c Q_b} & \sigma^2_{Q_c} & \sigma_{Q_c Q_d} \\ \sigma_{Q_d Q_a} & \sigma_{Q_d Q_b} & \sigma_{Q_d Q_c} & \sigma^2_{Q_d} \end{bmatrix}, \end{aligned} \tag{13}$$

where σ_{XY} denotes the covariance between the scalar components of the vector and σ^2_X denotes the variance of the vector component.

For an augmented quaternion as a random variable of the form $\overrightarrow{Q^a} = [Q, Q^\imath, Q^\jmath, Q^\kappa]^T$, the covariance matrix C^a can be determined as the expected value $E\{\cdot\}$ of the product $\overrightarrow{Q^a} \cdot \overrightarrow{Q^{aH}}$. The augmented quaternion valued covariance matrix C^a is [52], [69]

$$\begin{aligned} C^a &= E\{\overrightarrow{Q^a} \cdot \overrightarrow{Q^{aH}}\} = E\{A \cdot \overrightarrow{Q} \cdot \overrightarrow{Q}^H \cdot A^H\} \\ &= A \cdot E\{\overrightarrow{Q} \cdot \overrightarrow{Q}^H\} \cdot A^H = A \cdot C \cdot A^H. \end{aligned} \tag{14}$$

It can be noticed that the matrix C^a depends on the matrix C. The inverse of the transformation (14) where the real valued quadrivariate covariance matrix depends on the augmented quaternion valued covariance matrix can be represented by [52] and [69]

$$C = A^{-1} \cdot C^a \cdot A^{-H} \tag{15}$$

and taking into account (9) and (10), (15) can be rewritten as [52]

$$C = \frac{1}{16} A^H \cdot C^a \cdot A. \tag{16}$$

The inverse matrix C^{-1} is found from (15)

$$C^{-1} = A^H \cdot \left(C^a\right)^{-1} \cdot A. \tag{17}$$

Based on (17), the inverse of the augmented quaternion valued covariance matrix expressed in terms of the real valued quadrivariate covariance matrix is

$$\left(C^a\right)^{-1} = A^{-H} \cdot C^{-1} \cdot A^{-1} \tag{18}$$

and taking into account (9) and (10), (18) can be rewritten as

$$\left(C^a\right)^{-1} = \frac{1}{16} A \cdot C^{-1} \cdot A^H. \tag{19}$$

The determinant of C can be expressed as a function of C^a from (15) as [52] and [69]

$$|C| = |A^{-1} \cdot C^a \cdot A^{-H}| = |A^{-1}| \cdot |C^a| \cdot |A^{-H}| \tag{20}$$

and since $|A^{-1}| = |A|^{-1}$, and A^{-H} is given in (10), the above expression can be further simplified to

$$\begin{aligned} |C| &= |A|^{-1} \cdot |C^a| \cdot \left|\frac{1}{4} A\right| \\ &= |A|^{-1} \cdot |C^a| \cdot \left(\frac{1}{4}\right)^4 \cdot |A| \\ &= \left(\frac{1}{16}\right)^2 \cdot |C^a|, \end{aligned} \tag{21}$$

where $|A|$ is given in (12).

The structure of the augmented covariance matrix C^a can be written in the form [52]

$$C^a = \begin{bmatrix} \sigma_{QQ^*} & \sigma_{QQ^{\imath *}} & \sigma_{QQ^{\jmath *}} & \sigma_{QQ^{\kappa *}} \\ \sigma_{Q^\imath Q^*} & \sigma_{Q^\imath Q^{\imath *}} & \sigma_{Q^\imath Q^{\jmath *}} & \sigma_{Q^\imath Q^{\kappa *}} \\ \sigma_{Q^\jmath Q^*} & \sigma_{Q^\jmath Q^{\imath *}} & \sigma_{Q^\jmath Q^{\jmath *}} & \sigma_{Q^\jmath Q^{\kappa *}} \\ \sigma_{Q^\kappa Q^*} & \sigma_{Q^\kappa Q^{\imath *}} & \sigma_{Q^\kappa Q^{\jmath *}} & \sigma_{Q^\kappa Q^{\kappa *}} \end{bmatrix}, \tag{22}$$

where $(\cdot)^*$ denotes a quaternion conjugate operator and where σ_{XY} denotes the quaternion-valued covariance between the quaternion components of the vector $\overrightarrow{Q^a}$ or the conjugate quaternion components of the vector $\overrightarrow{Q^a}$. Observe that the real and imaginary parts of each component of C^a (23)-(38) are linear functions of the real-valued variance and covariance between the scalar components of the vector $\overrightarrow{Q} = [Q_a, Q_b, Q_c, Q_d]^T$ [52].

$$\begin{aligned} \sigma_{QQ^*} = {} & (\sigma^2_{Q_a} + \sigma^2_{Q_b} + \sigma^2_{Q_c} + \sigma^2_{Q_d}) \\ & + (\sigma_{Q_bQ_a} - \sigma_{Q_aQ_b} - \sigma_{Q_cQ_d} + \sigma_{Q_dQ_c}) \cdot \imath \\ & + (\sigma_{Q_bQ_d} - \sigma_{Q_aQ_c} + \sigma_{Q_cQ_a} - \sigma_{Q_dQ_b}) \cdot \jmath \\ & + (\sigma_{Q_cQ_b} - \sigma_{Q_bQ_c} - \sigma_{Q_aQ_d} + \sigma_{Q_dQ_a}) \cdot \kappa \end{aligned} \tag{23}$$

$$\begin{aligned} \sigma_{QQ^{\imath *}} = {} & (\sigma^2_{Q_a} + \sigma^2_{Q_b} - \sigma^2_{Q_c} - \sigma^2_{Q_d}) \\ & + (\sigma_{Q_bQ_a} - \sigma_{Q_aQ_b} + \sigma_{Q_cQ_d} - \sigma_{Q_dQ_c}) \cdot \imath \\ & + (\sigma_{Q_aQ_c} - \sigma_{Q_bQ_d} + \sigma_{Q_cQ_a} - \sigma_{Q_dQ_b}) \cdot \jmath \\ & + (\sigma_{Q_aQ_d} + \sigma_{Q_bQ_c} + \sigma_{Q_cQ_b} + \sigma_{Q_dQ_a}) \cdot \kappa \end{aligned} \tag{24}$$

$$\begin{aligned} \sigma_{QQ^{\jmath *}} = {} & (\sigma^2_{Q_a} - \sigma^2_{Q_b} + \sigma^2_{Q_c} - \sigma^2_{Q_d}) \\ & + (\sigma_{Q_aQ_b} + \sigma_{Q_bQ_a} + \sigma_{Q_cQ_d} + \sigma_{Q_dQ_c}) \cdot \imath \\ & + (\sigma_{Q_cQ_a} - \sigma_{Q_bQ_d} - \sigma_{Q_aQ_c} + \sigma_{Q_dQ_b}) \cdot \jmath \\ & + (\sigma_{Q_aQ_d} - \sigma_{Q_bQ_c} - \sigma_{Q_cQ_b} + \sigma_{Q_dQ_a}) \cdot \kappa \end{aligned} \tag{25}$$

$$\begin{aligned} \sigma_{QQ^{\kappa *}} = {} & (\sigma^2_{Q_a} - \sigma^2_{Q_b} - \sigma^2_{Q_c} + \sigma^2_{Q_d}) \\ & + (\sigma_{Q_aQ_b} + \sigma_{Q_bQ_a} - \sigma_{Q_cQ_d} - \sigma_{Q_dQ_c}) \cdot \imath \\ & + (\sigma_{Q_aQ_c} + \sigma_{Q_bQ_d} + \sigma_{Q_cQ_a} + \sigma_{Q_dQ_b}) \cdot \jmath \\ & + (\sigma_{Q_bQ_c} - \sigma_{Q_aQ_d} - \sigma_{Q_cQ_b} + \sigma_{Q_dQ_a}) \cdot \kappa \end{aligned} \tag{26}$$

$$\begin{aligned} \sigma_{Q^\imath Q^*} = {} & (\sigma^2_{Q_a} + \sigma^2_{Q_b} - \sigma^2_{Q_c} - \sigma^2_{Q_d}) \\ & + (\sigma_{Q_bQ_a} - \sigma_{Q_aQ_b} + \sigma_{Q_cQ_d} - \sigma_{Q_dQ_c}) \cdot \imath \\ & + (\sigma_{Q_bQ_d} - \sigma_{Q_aQ_c} - \sigma_{Q_cQ_a} + \sigma_{Q_dQ_b}) \cdot \jmath \\ & + (-\sigma_{Q_aQ_d} - \sigma_{Q_bQ_c} - \sigma_{Q_cQ_b} - \sigma_{Q_dQ_a}) \cdot \kappa \end{aligned} \tag{27}$$

$$\begin{aligned} \sigma_{Q^\imath Q^{\imath *}} = {} & (\sigma^2_{Q_a} + \sigma^2_{Q_b} + \sigma^2_{Q_c} + \sigma^2_{Q_d}) \\ & + (\sigma_{Q_bQ_a} - \sigma_{Q_aQ_b} - \sigma_{Q_cQ_d} + \sigma_{Q_dQ_c}) \cdot \imath \\ & + (\sigma_{Q_aQ_c} - \sigma_{Q_bQ_d} - \sigma_{Q_cQ_a} + \sigma_{Q_dQ_b}) \cdot \jmath \\ & + (\sigma_{Q_aQ_d} + \sigma_{Q_bQ_c} - \sigma_{Q_cQ_b} - \sigma_{Q_dQ_a}) \cdot \kappa \end{aligned} \tag{28}$$

$$\begin{aligned} \sigma_{Q^\imath Q^{\jmath *}} = {} & (\sigma^2_{Q_a} - \sigma^2_{Q_b} - \sigma^2_{Q_c} + \sigma^2_{Q_d}) \\ & + (\sigma_{Q_aQ_b} + \sigma_{Q_bQ_a} - \sigma_{Q_cQ_d} - \sigma_{Q_dQ_c}) \cdot \imath \\ & + (-\sigma_{Q_aQ_c} - \sigma_{Q_bQ_d} - \sigma_{Q_cQ_a} - \sigma_{Q_dQ_b}) \cdot \jmath \\ & + (\sigma_{Q_aQ_d} - \sigma_{Q_bQ_c} + \sigma_{Q_cQ_b} - \sigma_{Q_dQ_a}) \cdot \kappa \end{aligned} \tag{29}$$

$$\begin{aligned} \sigma_{Q^\imath Q^{\kappa *}} = {} & (\sigma^2_{Q_a} - \sigma^2_{Q_b} + \sigma^2_{Q_c} - \sigma^2_{Q_d}) \\ & + (\sigma_{Q_aQ_b} + \sigma_{Q_bQ_a} + \sigma_{Q_cQ_d} + \sigma_{Q_dQ_c}) \cdot \imath \\ & + (\sigma_{Q_aQ_c} + \sigma_{Q_bQ_d} - \sigma_{Q_cQ_a} - \sigma_{Q_dQ_b}) \cdot \jmath \\ & + (\sigma_{Q_bQ_c} - \sigma_{Q_aQ_d} + \sigma_{Q_cQ_b} - \sigma_{Q_dQ_a}) \cdot \kappa \end{aligned} \tag{30}$$

$$\begin{aligned} \sigma_{Q^\jmath Q^*} = {} & (\sigma^2_{Q_a} - \sigma^2_{Q_b} + \sigma^2_{Q_c} - \sigma^2_{Q_d}) \\ & + (-\sigma_{Q_aQ_b} - \sigma_{Q_bQ_a} - \sigma_{Q_cQ_d} - \sigma_{Q_dQ_c}) \cdot \imath \\ & + (\sigma_{Q_cQ_a} - \sigma_{Q_bQ_d} - \sigma_{Q_aQ_c} + \sigma_{Q_dQ_b}) \cdot \jmath \\ & + (\sigma_{Q_bQ_c} - \sigma_{Q_aQ_d} + \sigma_{Q_cQ_b} - \sigma_{Q_dQ_a}) \cdot \kappa \end{aligned} \tag{31}$$

$$\begin{aligned} \sigma_{Q^\jmath Q^{\imath *}} = {} & (\sigma^2_{Q_a} - \sigma^2_{Q_b} - \sigma^2_{Q_c} + \sigma^2_{Q_d}) \\ & + (\sigma_{Q_cQ_d} - \sigma_{Q_bQ_a} - \sigma_{Q_aQ_b} + \sigma_{Q_dQ_c}) \cdot \imath \\ & + (\sigma_{Q_aQ_c} + \sigma_{Q_bQ_d} + \sigma_{Q_cQ_a} + \sigma_{Q_dQ_b}) \cdot \jmath \\ & + (\sigma_{Q_aQ_d} - \sigma_{Q_bQ_c} + \sigma_{Q_cQ_b} - \sigma_{Q_dQ_a}) \cdot \kappa \end{aligned} \tag{32}$$

$$\begin{aligned} \sigma_{Q^\jmath Q^{\jmath *}} = {} & (\sigma^2_{Q_a} + \sigma^2_{Q_b} + \sigma^2_{Q_c} + \sigma^2_{Q_d}) \\ & + (\sigma_{Q_aQ_b} - \sigma_{Q_bQ_a} + \sigma_{Q_cQ_d} - \sigma_{Q_dQ_c}) \cdot \imath \\ & + (\sigma_{Q_bQ_d} - \sigma_{Q_aQ_c} + \sigma_{Q_cQ_a} - \sigma_{Q_dQ_b}) \cdot \jmath \\ & + (\sigma_{Q_aQ_d} + \sigma_{Q_bQ_c} - \sigma_{Q_cQ_b} - \sigma_{Q_dQ_a}) \cdot \kappa \end{aligned} \tag{33}$$

$$\begin{aligned} \sigma_{Q^\jmath Q^{\kappa *}} = {} & (\sigma^2_{Q_a} + \sigma^2_{Q_b} - \sigma^2_{Q_c} - \sigma^2_{Q_d}) \\ & + (\sigma_{Q_aQ_b} - \sigma_{Q_bQ_a} - \sigma_{Q_cQ_d} + \sigma_{Q_dQ_c}) \cdot \imath \\ & + (\sigma_{Q_aQ_c} - \sigma_{Q_bQ_d} + \sigma_{Q_cQ_a} - \sigma_{Q_dQ_b}) \cdot \jmath \\ & + (-\sigma_{Q_aQ_d} - \sigma_{Q_bQ_c} - \sigma_{Q_cQ_b} - \sigma_{Q_dQ_a}) \cdot \kappa \end{aligned} \tag{34}$$

$$\begin{aligned} \sigma_{Q^\kappa Q^*} = {} & (\sigma^2_{Q_a} - \sigma^2_{Q_b} - \sigma^2_{Q_c} + \sigma^2_{Q_d}) \\ & + (\sigma_{Q_cQ_d} - \sigma_{Q_bQ_a} - \sigma_{Q_aQ_b} + \sigma_{Q_dQ_c}) \cdot \imath \\ & + (-\sigma_{Q_aQ_c} - \sigma_{Q_bQ_d} - \sigma_{Q_cQ_a} - \sigma_{Q_dQ_b}) \cdot \jmath \\ & + (\sigma_{Q_bQ_c} - \sigma_{Q_aQ_d} - \sigma_{Q_cQ_b} + \sigma_{Q_dQ_a}) \cdot \kappa \end{aligned} \tag{35}$$

$$\begin{aligned} \sigma_{Q^\kappa Q^{\imath *}} = {} & (\sigma^2_{Q_a} - \sigma^2_{Q_b} + \sigma^2_{Q_c} - \sigma^2_{Q_d}) \\ & + (-\sigma_{Q_aQ_b} - \sigma_{Q_bQ_a} - \sigma_{Q_cQ_d} - \sigma_{Q_dQ_c}) \cdot \imath \\ & + (\sigma_{Q_aQ_c} + \sigma_{Q_bQ_d} - \sigma_{Q_cQ_a} - \sigma_{Q_dQ_b}) \cdot \jmath \\ & + (\sigma_{Q_aQ_d} - \sigma_{Q_bQ_c} - \sigma_{Q_cQ_b} + \sigma_{Q_dQ_a}) \cdot \kappa \end{aligned} \tag{36}$$

$$\begin{aligned} \sigma_{Q^\kappa Q^{\jmath *}} = {} & (\sigma^2_{Q_a} + \sigma^2_{Q_b} - \sigma^2_{Q_c} - \sigma^2_{Q_d}) \\ & + (\sigma_{Q_aQ_b} - \sigma_{Q_bQ_a} - \sigma_{Q_cQ_d} + \sigma_{Q_dQ_c}) \cdot \imath \\ & + (\sigma_{Q_bQ_d} - \sigma_{Q_aQ_c} - \sigma_{Q_cQ_a} + \sigma_{Q_dQ_b}) \cdot \jmath \\ & + (\sigma_{Q_aQ_d} + \sigma_{Q_bQ_c} + \sigma_{Q_cQ_b} + \sigma_{Q_dQ_a}) \cdot \kappa \end{aligned} \tag{37}$$

$$\begin{aligned} \sigma_{Q^\kappa Q^{\kappa *}} = {} & (\sigma^2_{Q_a} + \sigma^2_{Q_b} + \sigma^2_{Q_c} + \sigma^2_{Q_d}) \\ & + (\sigma_{Q_aQ_b} - \sigma_{Q_bQ_a} + \sigma_{Q_cQ_d} - \sigma_{Q_dQ_c}) \cdot \imath \\ & + (\sigma_{Q_aQ_c} - \sigma_{Q_bQ_d} - \sigma_{Q_cQ_a} + \sigma_{Q_dQ_b}) \cdot \jmath \\ & + (\sigma_{Q_cQ_b} - \sigma_{Q_bQ_c} - \sigma_{Q_aQ_d} + \sigma_{Q_dQ_a}) \cdot \kappa \end{aligned} \tag{38}$$

The quaternion-valued covariance components of the augmented covariance matrix C^a satisfy the following relationships

$$\sigma_{Q^\imath Q^*} = \left(\sigma_{QQ^{\imath *}}\right)^{\imath}, \tag{39}$$

$$\sigma_{Q^\jmath Q^*} = \left(\sigma_{QQ^{\jmath *}}\right)^{\jmath}, \tag{40}$$

$$\sigma_{Q^\kappa Q^*} = \left(\sigma_{QQ^{\kappa *}}\right)^{\kappa}, \tag{41}$$

$$\sigma_{Q^\jmath Q^{\imath *}} = \left(\sigma_{Q^\imath Q^{\jmath *}}\right)^{\imath\jmath}, \tag{42}$$

$$\sigma_{Q^\kappa Q^{\imath *}} = \left(\sigma_{Q^\imath Q^{\kappa *}}\right)^{\imath\kappa}, \tag{43}$$

$$\sigma_{Q^\kappa Q^{\jmath *}} = \left(\sigma_{Q^\jmath Q^{\kappa *}}\right)^{\jmath\kappa}. \tag{44}$$

If the covariance between the scalar components of the vector $\overrightarrow{Q}$ satisfies the condition $\sigma_{XY} = \sigma_{YX}$, where

$X, Y \in \{Q_a, Q_b, Q_c, Q_d\}$ and $X \neq Y$, then the structure of C^a is reduced and (23)-(38) can be rewritten as (45)-(60).

$$\sigma_{QQ^*} = \sigma_{Q_a}^2 + \sigma_{Q_b}^2 + \sigma_{Q_c}^2 + \sigma_{Q_d}^2 \tag{45}$$

$$\begin{aligned}\sigma_{QQ^{\imath*}} &= (\sigma_{Q_a}^2 + \sigma_{Q_b}^2 - \sigma_{Q_c}^2 - \sigma_{Q_d}^2) \\ &+ (2 \cdot \sigma_{Q_aQ_c} - 2 \cdot \sigma_{Q_bQ_d}) \cdot \jmath \\ &+ (2 \cdot \sigma_{Q_aQ_d} + 2 \cdot \sigma_{Q_bQ_c}) \cdot \kappa\end{aligned} \tag{46}$$

$$\begin{aligned}\sigma_{QQ^{\jmath*}} &= (\sigma_{Q_a}^2 - \sigma_{Q_b}^2 + \sigma_{Q_c}^2 - \sigma_{Q_d}^2) \\ &+ (2 \cdot \sigma_{Q_aQ_b} + 2 \cdot \sigma_{Q_cQ_d}) \cdot \imath \\ &+ (2 \cdot \sigma_{Q_aQ_d} - 2 \cdot \sigma_{Q_bQ_c}) \cdot \kappa\end{aligned} \tag{47}$$

$$\begin{aligned}\sigma_{QQ^{\kappa*}} &= (\sigma_{Q_a}^2 - \sigma_{Q_b}^2 - \sigma_{Q_c}^2 + \sigma_{Q_d}^2) \\ &+ (2 \cdot \sigma_{Q_aQ_b} - 2 \cdot \sigma_{Q_cQ_d}) \cdot \imath \\ &+ (2 \cdot \sigma_{Q_aQ_c} + 2 \cdot \sigma_{Q_bQ_d}) \cdot \jmath\end{aligned} \tag{48}$$

$$\begin{aligned}\sigma_{Q^\imath Q^*} &= (\sigma_{Q_a}^2 + \sigma_{Q_b}^2 - \sigma_{Q_c}^2 - \sigma_{Q_d}^2) \\ &+ (2 \cdot \sigma_{Q_bQ_d} - 2 \cdot \sigma_{Q_aQ_c}) \cdot \jmath \\ &+ (-2 \cdot \sigma_{Q_aQ_d} - 2 \cdot \sigma_{Q_bQ_c}) \cdot \kappa\end{aligned} \tag{49}$$

$$\sigma_{Q^\imath Q^{\imath*}} = \sigma_{Q_a}^2 + \sigma_{Q_b}^2 + \sigma_{Q_c}^2 + \sigma_{Q_d}^2 \tag{50}$$

$$\begin{aligned}\sigma_{Q^\imath Q^{\jmath*}} &= (\sigma_{Q_a}^2 - \sigma_{Q_b}^2 - \sigma_{Q_c}^2 + \sigma_{Q_d}^2) \\ &+ (2 \cdot \sigma_{Q_aQ_b} - 2 \cdot \sigma_{Q_cQ_d}) \cdot \imath \\ &+ (-2 \cdot \sigma_{Q_aQ_c} - 2 \cdot \sigma_{Q_bQ_d}) \cdot \jmath\end{aligned} \tag{51}$$

$$\begin{aligned}\sigma_{Q^\imath Q^{\kappa*}} &= (\sigma_{Q_a}^2 - \sigma_{Q_b}^2 + \sigma_{Q_c}^2 - \sigma_{Q_d}^2) \\ &+ (2 \cdot \sigma_{Q_aQ_b} + 2 \cdot \sigma_{Q_cQ_d}) \cdot \imath \\ &+ (2 \cdot \sigma_{Q_bQ_c} - 2 \cdot \sigma_{Q_aQ_d}) \cdot \kappa\end{aligned} \tag{52}$$

$$\begin{aligned}\sigma_{Q^\jmath Q^*} &= (\sigma_{Q_a}^2 - \sigma_{Q_b}^2 + \sigma_{Q_c}^2 - \sigma_{Q_d}^2) \\ &+ (-2 \cdot \sigma_{Q_aQ_b} - 2 \cdot \sigma_{Q_cQ_d}) \cdot \imath \\ &+ (2 \cdot \sigma_{Q_bQ_c} - 2 \cdot \sigma_{Q_aQ_d}) \cdot \kappa\end{aligned} \tag{53}$$

$$\begin{aligned}\sigma_{Q^\jmath Q^{\imath*}} &= (\sigma_{Q_a}^2 - \sigma_{Q_b}^2 - \sigma_{Q_c}^2 + \sigma_{Q_d}^2) \\ &+ (2 \cdot \sigma_{Q_cQ_d} - 2 \cdot \sigma_{Q_aQ_b}) \cdot \imath \\ &+ (2 \cdot \sigma_{Q_aQ_c} + 2 \cdot \sigma_{Q_bQ_d}) \cdot \jmath\end{aligned} \tag{54}$$

$$\sigma_{Q^\jmath Q^{\jmath*}} = \sigma_{Q_a}^2 + \sigma_{Q_b}^2 + \sigma_{Q_c}^2 + \sigma_{Q_d}^2 \tag{55}$$

$$\begin{aligned}\sigma_{Q^\jmath Q^{\kappa*}} &= (\sigma_{Q_a}^2 + \sigma_{Q_b}^2 - \sigma_{Q_c}^2 - \sigma_{Q_d}^2) \\ &+ (2 \cdot \sigma_{Q_aQ_c} - 2 \cdot \sigma_{Q_bQ_d}) \cdot \jmath \\ &+ (-2 \cdot \sigma_{Q_aQ_d} - 2 \cdot \sigma_{Q_bQ_c}) \cdot \kappa\end{aligned} \tag{56}$$

$$\begin{aligned}\sigma_{Q^\kappa Q^*} &= (\sigma_{Q_a}^2 - \sigma_{Q_b}^2 - \sigma_{Q_c}^2 + \sigma_{Q_d}^2) \\ &+ (2 \cdot \sigma_{Q_cQ_d} - 2 \cdot \sigma_{Q_aQ_b}) \cdot \imath \\ &+ (-2 \cdot \sigma_{Q_aQ_c} - 2 \cdot \sigma_{Q_bQ_d}) \cdot \jmath\end{aligned} \tag{57}$$

$$\begin{aligned}\sigma_{Q^\kappa Q^{\imath*}} &= (\sigma_{Q_a}^2 - \sigma_{Q_b}^2 + \sigma_{Q_c}^2 - \sigma_{Q_d}^2) \\ &+ (-2 \cdot \sigma_{Q_aQ_b} - 2 \cdot \sigma_{Q_cQ_d}) \cdot \imath \\ &+ (2 \cdot \sigma_{Q_aQ_d} - 2 \cdot \sigma_{Q_bQ_c}) \cdot \kappa\end{aligned} \tag{58}$$

$$\begin{aligned}\sigma_{Q^\kappa Q^{\jmath*}} &= (\sigma_{Q_a}^2 + \sigma_{Q_b}^2 - \sigma_{Q_c}^2 - \sigma_{Q_d}^2) \\ &+ (2 \cdot \sigma_{Q_bQ_d} - 2 \cdot \sigma_{Q_aQ_c}) \cdot \jmath \\ &+ (2 \cdot \sigma_{Q_aQ_d} + 2 \cdot \sigma_{Q_bQ_c}) \cdot \kappa\end{aligned} \tag{59}$$

$$\sigma_{Q^\kappa Q^{\kappa*}} = \sigma_{Q_a}^2 + \sigma_{Q_b}^2 + \sigma_{Q_c}^2 + \sigma_{Q_d}^2 \tag{60}$$

For (45)-(60), the augmented covariance matrix satisfies the $C^a = (C^a)^H$ condition.

The real-valued variance of each single component Q_a, Q_b, Q_c and Q_d of the random quaternion $\overrightarrow{Q}$ and the real-valued covariance between each component Q_a, Q_b, Q_c and Q_d can be expressed in terms of the quaternion-valued covariance [52], that is

$$\sigma_{Q_a}^2 = \frac{1}{4}\Re\left\{\sigma_{QQ^*} + \sigma_{QQ^{\imath*}} + \sigma_{QQ^{\jmath*}} + \sigma_{QQ^{\kappa*}}\right\}, \tag{61}$$

$$\sigma_{Q_bQ_a} = \frac{1}{4}\Im_\imath\left\{\sigma_{QQ^*} + \sigma_{QQ^{\imath*}} + \sigma_{QQ^{\jmath*}} + \sigma_{QQ^{\kappa*}}\right\}, \tag{62}$$

$$\sigma_{Q_cQ_a} = \frac{1}{4}\Im_\jmath\left\{\sigma_{QQ^*} + \sigma_{QQ^{\imath*}} + \sigma_{QQ^{\jmath*}} + \sigma_{QQ^{\kappa*}}\right\}, \tag{63}$$

$$\sigma_{Q_dQ_a} = \frac{1}{4}\Im_\kappa\left\{\sigma_{QQ^*} + \sigma_{QQ^{\imath*}} + \sigma_{QQ^{\jmath*}} + \sigma_{QQ^{\kappa*}}\right\}, \tag{64}$$

$$\sigma_{Q_b}^2 = \frac{1}{4}\Re\left\{\sigma_{QQ^*} + \sigma_{QQ^{\imath*}} - \sigma_{QQ^{\jmath*}} - \sigma_{QQ^{\kappa*}}\right\}, \tag{65}$$

$$\sigma_{Q_aQ_b} = -\frac{1}{4}\Im_\imath\left\{\sigma_{QQ^*} + \sigma_{QQ^{\imath*}} - \sigma_{QQ^{\jmath*}} - \sigma_{QQ^{\kappa*}}\right\}, \tag{66}$$

$$\sigma_{Q_dQ_b} = -\frac{1}{4}\Im_\jmath\left\{\sigma_{QQ^*} + \sigma_{QQ^{\imath*}} - \sigma_{QQ^{\jmath*}} - \sigma_{QQ^{\kappa*}}\right\}, \tag{67}$$

$$\sigma_{Q_cQ_b} = \frac{1}{4}\Im_\kappa\left\{\sigma_{QQ^*} + \sigma_{QQ^{\imath*}} - \sigma_{QQ^{\jmath*}} - \sigma_{QQ^{\kappa*}}\right\}, \tag{68}$$

$$\sigma_{Q_c}^2 = \frac{1}{4}\Re\left\{\sigma_{QQ^*} - \sigma_{QQ^{\imath*}} + \sigma_{QQ^{\jmath*}} - \sigma_{QQ^{\kappa*}}\right\}, \tag{69}$$

$$\sigma_{Q_dQ_c} = \frac{1}{4}\Im_\imath\left\{\sigma_{QQ^*} - \sigma_{QQ^{\imath*}} + \sigma_{QQ^{\jmath*}} - \sigma_{QQ^{\kappa*}}\right\}, \tag{70}$$

$$\sigma_{Q_aQ_c} = -\frac{1}{4}\Im_\jmath\left\{\sigma_{QQ^*} - \sigma_{QQ^{\imath*}} + \sigma_{QQ^{\jmath*}} - \sigma_{QQ^{\kappa*}}\right\}, \tag{71}$$

$$\sigma_{Q_bQ_c} = -\frac{1}{4}\Im_\kappa\left\{\sigma_{QQ^*} - \sigma_{QQ^{\imath*}} + \sigma_{QQ^{\jmath*}} - \sigma_{QQ^{\kappa*}}\right\}, \tag{72}$$

$$\sigma_{Q_d}^2 = \frac{1}{4}\Re\left\{\sigma_{QQ^*} - \sigma_{QQ^{\imath*}} - \sigma_{QQ^{\jmath*}} + \sigma_{QQ^{\kappa*}}\right\}, \tag{73}$$

$$\sigma_{Q_cQ_d} = -\frac{1}{4}\Im_\imath\left\{\sigma_{QQ^*} - \sigma_{QQ^{\imath*}} - \sigma_{QQ^{\jmath*}} + \sigma_{QQ^{\kappa*}}\right\}, \tag{74}$$

$$\sigma_{Q_bQ_d} = \frac{1}{4}\Im_\jmath\left\{\sigma_{QQ^*} - \sigma_{QQ^{\imath*}} - \sigma_{QQ^{\jmath*}} + \sigma_{QQ^{\kappa*}}\right\}, \tag{75}$$

$$\sigma_{Q_aQ_d} = -\frac{1}{4}\Im_\kappa\left\{\sigma_{QQ^*} - \sigma_{QQ^{\imath*}} - \sigma_{QQ^{\jmath*}} + \sigma_{QQ^{\kappa*}}\right\}, \tag{76}$$

where $\Im_{\imath,\jmath,\kappa}\{\cdot\}$ denotes the $\imath$-, $\jmath$-, κ-component of the vector imaginary part of the quaternion and $\Re\{\cdot\}$ denotes the scalar real part q_a of the quaternion.

B. MGGD

The probability density function of a zero-mean MGGD in $\mathbb{R}^d$ is defined by [45] and [71]

$$\begin{aligned}f(\overrightarrow{x}|d, M, p) = &\frac{p \cdot \Gamma(d/2)}{\pi^{d/2} \cdot \Gamma(d/(2p)) \cdot 2^{d/(2p)} \cdot \sqrt{|M|}} \cdot \\ &\cdot exp\left\{-\frac{1}{2} \cdot \left(\overrightarrow{x}^T M^{-1} \overrightarrow{x}\right)^p\right\}\end{aligned} \tag{77}$$

and

$$M = \frac{d \cdot \Gamma(d/(2p))}{2^{1/p} \cdot \Gamma((d+2)/(2p))} \cdot C \tag{78}$$

for any $\overrightarrow{x} \in \mathbb{R}^d$, where C is a $d \times d$ covariance matrix, d denotes the dimension of the probability space, $\overrightarrow{x}^T$ is the transpose of the vector $\overrightarrow{x}$, p is the shape parameter of MGGD, $\Gamma(\cdot)$ is the gamma function $\Gamma(z) = \int_0^\infty t^{z-1}e^{-t}dt, z > 0$ [4].

The special cases with the exponents $p = 1$ and $p = 0.5$ cover the multivariate Gaussian distribution (MGD) and the multivariate Laplacian distribution (MLD), respectively. For $p \to \infty$, the MGGD density function becomes a multivariate uniform distribution [40], [42].

The p parameter of the MGGD distribution can be determined using the ML method [42], [43], [72]

$$\frac{d}{2} \cdot \frac{\sum_{i=1}^N u_i^p \cdot \log(u_i)}{\sum_{i=1}^N u_i^p} - \frac{d}{2p} \cdot \left[\Psi\left(\frac{d}{2p}\right) + \log(2)\right] - 1 - \frac{d}{2p} \cdot \log\left(\frac{p}{d \cdot N} \sum_{i=1}^N u_i^p\right) = 0, \tag{79}$$

where $u_i = \overrightarrow{x_i}^T C^{-1} \overrightarrow{x_i}$ and $\Psi(x) = \frac{d}{dx} log\big(\Gamma(x)\big)$ is digamma function [4], and $\{\overrightarrow{x_1}, \overrightarrow{x_2}, \ldots, \overrightarrow{x_N}\}$ is a random sample of N observation vectors of dimension d. The nonlinear equation (79) must be solved numerically in terms of p assuming that C is known.

Whereas, the ML estimate $\hat{C}$ is the solution of the following equation [42], [43]

$$C = \sum_{i=1}^N \frac{d}{u_i + u_i^{1-p} \sum_{j \neq i} u_j^p} \overrightarrow{x_i}\, \overrightarrow{x_i}^T \tag{80}$$

for unknown C and assuming that p is known. In the general case, both (79) and (80) must be solved simultaneously due to the determination of the p parameter and the C parameter.

Equation (79) for $d = 1$ after appropriate transformations can be reduced to the form (2).

C. 3D GGD

The probability density function of a zero-mean 3D GGD is [69]

$$f_X(\overrightarrow{x}) = \frac{p}{2\pi \cdot \sqrt{|C|} \cdot s^{\frac{3}{2p}} \Gamma\left(\frac{3}{2p}\right)} \cdot e^{-\frac{1}{s}\cdot(\overrightarrow{x}^T \cdot C^{-1} \cdot \overrightarrow{x})^p} \tag{81}$$

parameterized by the shape parameter p and the covariance matrix C, and the normalizing term is equal [69]

$$s = \left(\frac{3 \cdot \Gamma\left(\frac{3}{2p}\right)}{\Gamma\left(\frac{5}{2p}\right)}\right)^p. \tag{82}$$

Equation (81) is equal (77) for $d = 3$. The random variable $\overrightarrow{X} = [X_0, X_1, X_2]^T$ consists of three random variables X_0, X_1, and X_2 ($\overrightarrow{x} \in \mathbb{R}^3$). The random variable $\overrightarrow{X} = [X_0, X_1, X_2]^T$ corresponds to a pure quaternion random variable $\overrightarrow{Q_p} = [Q_b, Q_c, Q_d]^T$, where the real part is $Q_a = 0$.

This distribution was the starting point for creating GGD with an augmented quaternion random variable [69]

$$f(\overrightarrow{q^a}) = \frac{8p}{\pi \cdot \sqrt{|C^a|} \cdot s^{\frac{3}{2p}} \Gamma\left(\frac{3}{2p}\right)} \cdot e^{-\frac{1}{s}\cdot\left(\overrightarrow{q^a}^H \cdot (C^a)^{-1} \cdot \overrightarrow{q^a}\right)^p}. \tag{83}$$

This probability density function is parameterized by the shape parameter p and the augmented covariance matrix C^a. The connection of the augmented covariance matrix C^a with the original covariance matrix C is described by (16).

In the case of the random variable $\overrightarrow{Q} = [0, Q_b, Q_c, Q_d]^T$, which corresponds to a pure quaternion, a limiting case is obtained. Because the real valued quadrivariate covariance matrix C (13) is equal [69], [70]

$$C = \begin{bmatrix} 0 & 0 & 0 & 0 \\ 0 & \sigma_{Q_b}^2 & \sigma_{Q_bQ_c} & \sigma_{Q_bQ_d} \\ 0 & \sigma_{Q_cQ_b} & \sigma_{Q_c}^2 & \sigma_{Q_cQ_d} \\ 0 & \sigma_{Q_dQ_b} & \sigma_{Q_dQ_c} & \sigma_{Q_d}^2 \end{bmatrix}, \tag{84}$$

then the value of the determinant of the matrix C (84) is $|C| = 0$. According to (14), also $|C^a| = 0$. Since this value is in the denominator of (83), the limiting case for QGGD is obtained. Therefore, GGD for an augmented pure quaternion random variable is [70]

$$f(\overrightarrow{q_p^a}) = \frac{32p}{\pi \cdot \sqrt{|C_A|} \cdot s^{\frac{3}{2p}} \Gamma\left(\frac{3}{2p}\right)} \cdot e^{-\frac{1}{s}\cdot\left(\overrightarrow{q_p^a}^H \cdot A_p \cdot C_A^{-1} \cdot A_p^H \cdot \overrightarrow{q_p^a}\right)^p} \tag{85}$$

that is parameterized by the shape parameter p, s (82) and the matrix C_A (86) depends on the augmented covariance matrix C_p^a

$$C_A = A_p^H \cdot C_p^a \cdot A_p. \tag{86}$$

where

$$C_p^a = A_p \cdot C_p \cdot A_p^H. \tag{87}$$

$$C_p = \begin{bmatrix} \sigma_{Q_b}^2 & \sigma_{Q_bQ_c} & \sigma_{Q_bQ_d} \\ \sigma_{Q_cQ_b} & \sigma_{Q_c}^2 & \sigma_{Q_cQ_d} \\ \sigma_{Q_dQ_b} & \sigma_{Q_dQ_c} & \sigma_{Q_d}^2 \end{bmatrix}. \tag{88}$$

$$A_p = \begin{bmatrix} \imath & \jmath & \kappa \\ \imath & -\jmath & -\kappa \\ -\imath & \jmath & -\kappa \\ -\imath & -\jmath & \kappa \end{bmatrix} \tag{89}$$

The direct relationship between C_A and C_p is given in [70] as $C_A = 16 \cdot C_p$. The original covariance matrix C for GGD with an augmented pure quaternion random variable is represented by the matrix C_p of size 3×3. Whereas the dimension of the augmented covariance matrix C_p^a is 4×4.

The probability density function (85) is defined for a pure quaternion random variable $\overrightarrow{Q_p} = [Q_b, Q_c, Q_d]^T$, where

$$\overrightarrow{q_p^a} = A_p \cdot \overrightarrow{q_p}. \tag{90}$$

III. FULL QUATERNION GGD

Since a full quaternion has four components, 4D GGD will be used instead of 3D GGD (81) to create GGD for a full quaternion. Based on (77) and (78) for $d = 4$, a zero-mean GGD can be given for a full quaternion random variable $\overrightarrow{Q} = [Q_a, Q_b, Q_c, Q_d]^T$ as

$$f(\overrightarrow{q}) = \frac{p \cdot \Gamma^2(3/p)}{16\pi^2 \cdot \Gamma^3(2/p) \cdot \sqrt{|C|}} \cdot \cdot exp\left\{-\left(\frac{\Gamma(3/p)}{4\Gamma(2/p)}\right)^p \cdot \left(\overrightarrow{q}^T C^{-1} \overrightarrow{q}\right)^p\right\} \tag{91}$$

This probability density function is the basis for creating GGD with an augmented full quaternion random variable. In previous works, QGGD was based on 3D GGD.

The parameters of this distribution (91) can be determined using (79) and (80) for $d = 4$. Equation (79) simplifies to

$$\frac{1}{p} \cdot \Psi\left(\frac{2}{p}\right) + \frac{1}{2} + \frac{1}{p} \cdot \log\left(\frac{p}{2 \cdot N} \sum_{i=1}^{N} u_i^p\right) - \frac{\sum_{i=1}^{N} u_i^p \cdot \log(u_i)}{\sum_{i=1}^{N} u_i^p} = 0, \tag{92}$$

where $u_i = \overrightarrow{q_i}^T C^{-1} \overrightarrow{q_i}$ and $\{\overrightarrow{q_1}, \overrightarrow{q_2}, \ldots, \overrightarrow{q_N}\}$ is a random sample of N observation vectors of dimension 4. Both (92) and (80) must be solved simultaneously due to the determination of the p parameter and the C matrix.

IV. GGD WITH AN AUGMENTED FULL QUATERNION RANDOM VARIABLE

In (91), the dependence on C^a and $\overrightarrow{q^a}$ should be introduced instead of C and $\overrightarrow{q}$. The quadratic function $\overrightarrow{q}^T \cdot C^{-1} \cdot \overrightarrow{q}$, taking into account (8) and (17), can be written as [52] and [69]

$$\begin{aligned}\overrightarrow{q}^T \cdot C^{-1} \cdot \overrightarrow{q} &= \overrightarrow{q}^H \cdot C^{-1} \cdot \overrightarrow{q} \\ &= \overrightarrow{q}^H \cdot A^H \cdot (C^a)^{-1} \cdot A \cdot \overrightarrow{q} \\ &= \overrightarrow{q^a}^H \cdot (C^a)^{-1} \cdot \overrightarrow{q^a}.\end{aligned} \tag{93}$$

The equation for the generalized Gaussian probability density function for an augmented full quaternion random variable is obtained by substituting (21) and (93) into (91)

$$f(\overrightarrow{q^a}) = \frac{p \cdot \Gamma^2(3/p)}{\pi^2 \cdot \Gamma^3(2/p) \cdot \sqrt{|C^a|}} \cdot \cdot exp\left\{-\left(\frac{\Gamma(3/p)}{4\Gamma(2/p)}\right)^p \cdot \left(\overrightarrow{q^a}^H \cdot (C^a)^{-1} \cdot \overrightarrow{q^a}\right)^p\right\} \tag{94}$$

that is parameterized by the shape parameter p and the augmented covariance matrix C^a (14).

V. GGD WITH AN ℍ-PROPER QUATERNION RANDOM VARIABLE

Definition 1: (ℍ-properness) [49] A quaternion random variable q is said to be ℍ-proper if:

$$q \stackrel{d}{=} e^{\eta\phi} q, \forall \phi \tag{95}$$

and for any pure unit quaternion η.

An ℍ-proper quaternion random variable has a distribution that is invariant by left Clifford translation of axis η and of any angle ϕ.

In this case, the quaternion representations of the augmented covariance matrix have the following structure [49]:

$$C^a = 4\sigma_q^2 I_4, \tag{96}$$

where I_4 is the 4×4 identity matrix and

$$E\{Q_a^2\} = E\{Q_b^2\} = E\{Q_c^2\} = E\{Q_d^2\} = \sigma_q^2. \tag{97}$$

An ℍ-proper signal is uncorrelated with its perpendicular involutions and it also has uncorrelated components Q_a, Q_b, Q_c and Q_d that have equal variance σ_q^2. The distribution of an ℍ-proper quaternion random variable is invariant under any four dimensional isometric transformation.

The form of (96) can also be obtained by substituting (97) into (45)-(60).

Given (96), the determinant of the augmented quaternion valued covariance matrix C^a of an augmented quaternion random variable can be simplified to

$$|C^a| = \left(4\sigma_q^2\right)^4. \tag{98}$$

After rearranging (96), the inverse of the augmented quaternion valued covariance matrix is

$$\left(C^a\right)^{-1} = \frac{1}{4\sigma_q^2} I_4. \tag{99}$$

For an ℍ-proper random variable, it can be shown (using (98) and (99)) that QGGD (94) simplifies to

$$\begin{aligned}f(\overrightarrow{q^a} &= [q, q^\imath, q^\jmath, q^\kappa]^T) \\ &= \frac{p \cdot \Gamma^2(3/p)}{16\pi^2 \cdot \Gamma^3(2/p) \cdot \sigma_q^4} \\ &\quad \cdot exp\left\{-\left(\frac{\Gamma(3/p)}{4\sigma_q^2 \Gamma(2/p)}\right)^p \cdot \left(\overrightarrow{q}^T \overrightarrow{q}\right)^p\right\}\end{aligned} \tag{100}$$

that is parameterized by the shape parameter p. It should be noted that the parameter σ_q is not the standard deviation of the probability density function (100).

A. MAXIMUM LIKELIHOOD ESTIMATORS

The maximum likelihood estimator of the shape parameter p is obtained by differentiating the log-likelihood function of (100) with respect to p. The resulting equation, which has to be solved numerically, is given by

$$\frac{1}{p}\cdot\Psi\left(\frac{2}{p}\right)+\frac{1}{2}+\frac{1}{p}\cdot\log\left[\frac{p}{2\cdot N}\sum_{i=1}^{N}\left(\vec{q_i}^T\vec{q_i}\right)^p\right] - \frac{\sum_{i=1}^{N}\left(\vec{q_i}^T\vec{q_i}\right)^p\cdot\log\left(\vec{q_i}^T\vec{q_i}\right)}{\sum_{i=1}^{N}\left(\vec{q_i}^T\vec{q_i}\right)^p}=0. \tag{101}$$

The solution to (101) is the estimated value of $\hat{p}$. Note the similarity to (92), from which the dependence on the covariance matrix C has been removed.

The maximum likelihood estimator of the σ_q parameter is obtained by differentiating the log-likelihood function of (100) with respect to σ_q. The resulting equation is given by

$$\hat{\sigma_q}=0.5\left(\frac{\Gamma(3/p)}{\Gamma(2/p)}\right)^{0.5}\left[\frac{p}{2N}\sum_{i=1}^{N}\left(\vec{q_i}^T\vec{q_i}\right)^p\right]^{1/(2p)}, \tag{102}$$

where $\hat{\sigma_q}$ denotes the estimated value. The found p value from (101) is substituted into (102) to determine $\hat{\sigma_q}$.

An equation with the same form as (101) can be obtained using (92) and the information that the quaternion representations of the covariance matrix have the following structure [49]

$$C=\sigma_q^2 I_4 \tag{103}$$

for an ℍ-proper quaternion random variable.

VI. SIMULATIONS

The relative mean square error (RMSE) was used to evaluate the performance of the introduced estimators. RMSE was calculated from the equation

$$RMSE=\frac{1}{M}\sum_{i=1}^{M}\frac{(\hat{x}_i-x)^2}{x^2}, \tag{104}$$

where $\hat{x}_i$ is an estimated value ($\hat{p}$ or $\hat{\sigma_q}$) by the ML method and x is a real value (p or σ_q). M denotes the number of repetitions and was set to $M=10^4$ for all experiments.

First, the value of the shape parameter $\hat{p}$ was determined from (101). Then the found $\hat{p}$ value was substituted into (102) and the $\hat{\sigma_q}$ value was determined. The experiment was repeated M times and for the determined values of $\hat{p}_i$ and $\hat{\sigma_q}_i$, p RMSE and σ_q RMSE were calculated, respectively.

Equations (101) and (102) from the article were validated with the MGGD generator [40], [42] with the fixed parameter $\sigma_q=0.5$ or $\sigma_q=5$ and varying shape parameter in the range $p \in< 0.3, 8 >$. The range of the p parameter was chosen as the most common range in the literature when modeling signals with the use of GGD. The vector size N was set to $5\cdot10^4$. Since σ_q^2 corresponds to the variance of the Q_a, Q_b, Q_c, and Q_d components, Figs. 1 and 2 have been prepared for the lower variance $\sigma_q^2=0.5^2$ and the relatively higher value $\sigma_q^2=5^2$ of the variance.

Fig. 1 shows that as the value of the shape parameter p increases, RMSE of the shape parameter estimator also increases. However, whether it is $\sigma_q=0.5$ or $\sigma_q=5$, it does not significantly affect p RMSE.

In the case of the σ_q parameter, RMSE of the σ_q parameter estimator decreases with the increasing value of the shape parameter p (Fig. 2). Also in this case, whether it is $\sigma_q=0.5$ or $\sigma_q=5$, it does not significantly affect σ_q RMSE.

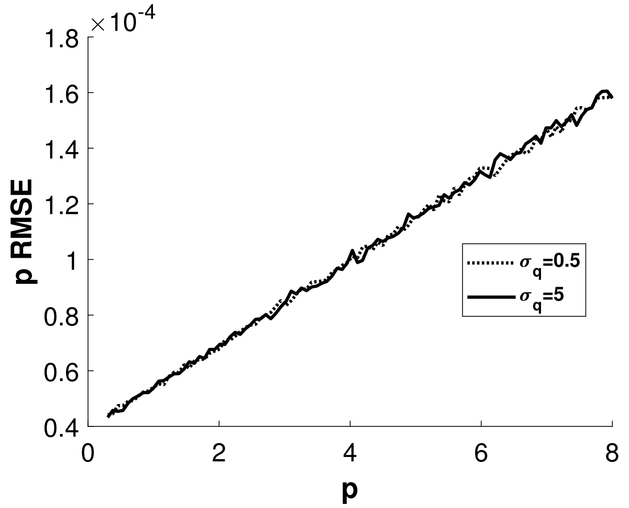

FIGURE 1. Comparison of RMSE for the ML method of the estimation of the shape parameter p (101) of QGGD with a varying shape value p and the selected fixed values $\sigma_q=0.5$ and $\sigma_q=5$ in the MGGD generator.

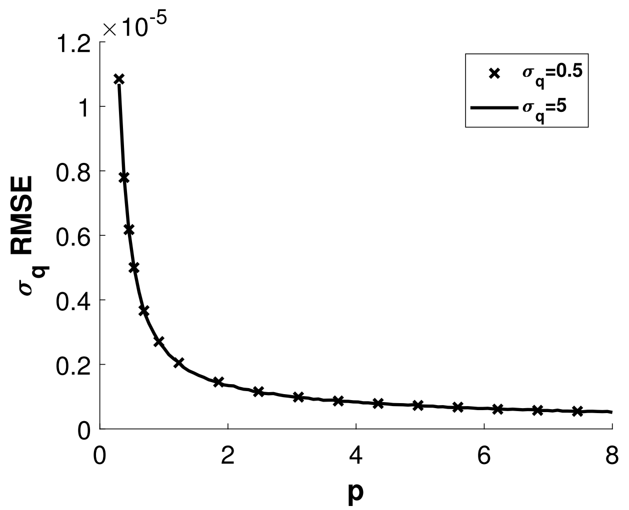

FIGURE 2. Comparison of RMSE for the ML method of the estimation of the σ_q parameter (102) of QGGD with a varying shape value p and the selected fixed value $\sigma_q=0.5$ and $\sigma_q=5$ in the MGGD generator.

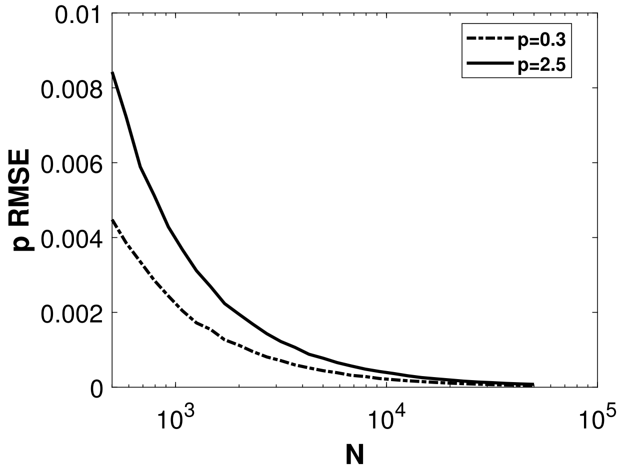

FIGURE 3. Comparison of RMSE for the ML method of the estimation of the shape parameter p (101) of QGGD with a varying sample size N and the selected fixed value $\sigma_q = 1$ in the MGGD generator for $p = 0.3$ and $p = 2.5$.

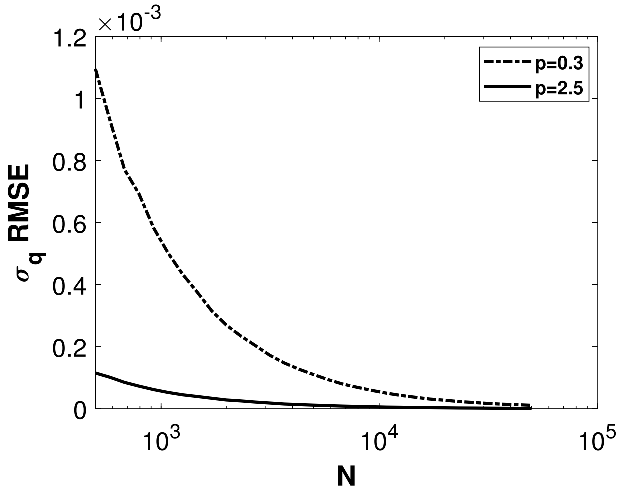

FIGURE 4. Comparison of RMSE for the ML method of the estimation of the σ_q parameter (102) of QGGD with a varying sample size N and the selected fixed value $\sigma_q = 1$ in the MGGD generator for $p = 0.3$ and $p = 2.5$.

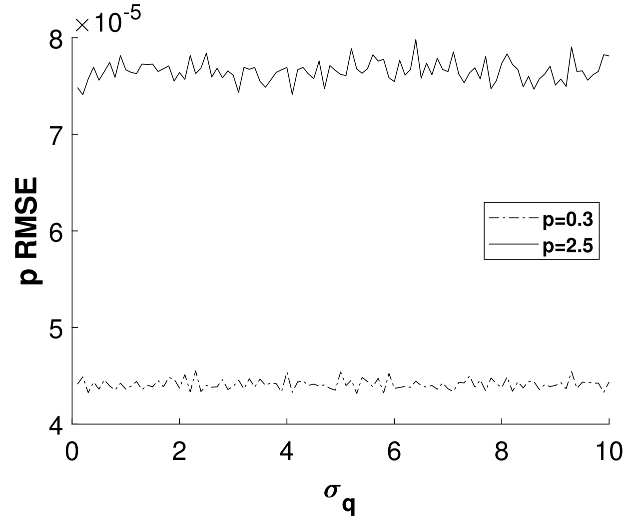

FIGURE 5. Comparison of RMSE for the ML method of the estimation of the shape parameter p (101) of QGGD with a varying σ_q parameter and the selected fixed shape value $p = 0.3$ and $p = 2.5$ in the MGGD generator.

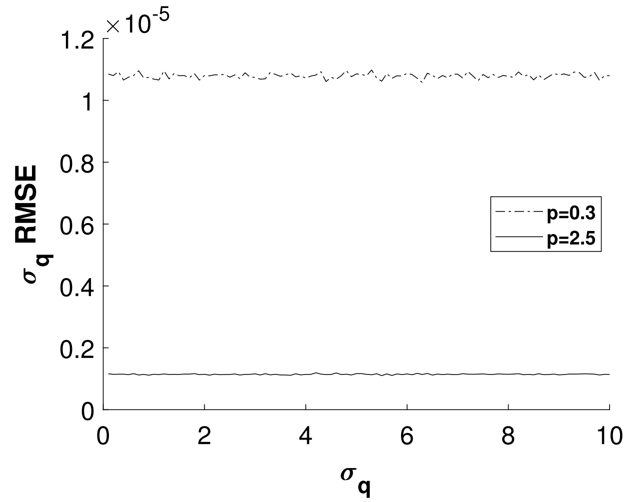

FIGURE 6. Comparison of RMSE for the ML method of the estimation of the σ_q parameter (102) of QGGD with a varying σ_q parameter and the selected fixed shape value $p = 0.3$ and $p = 2.5$ in the MGGD generator.

In the next step, the influence of the sample size N on the RMSE value was examined. The range of changes of the parameter N has been set to $5 \cdot 10^2$ to $5 \cdot 10^4$. The value of the parameter σ_q has been set to a fixed value of 1. As expected, the accuracy of the ML estimators decreases with decreasing sample size. Therefore, large sample sizes are recommended for the ML estimators. The results are shown in Figs. 3 and 4.

According to Fig. 3, for small sample sizes, for a more impulsive distribution $p = 0.3$, the ML estimator of parameter p has a smaller RMSE error than for a distribution with $p = 2.5$. The opposite behavior is observed for RMSE of the σ_q estimator (Fig. 4). The σ_q RMSE values for the more impulsive distribution $p = 0.3$ are larger than those for the distribution $p = 2.5$.

Additionally, (101) and (102) were validated with the MGGD generator with the fixed shape parameter $p = 0.3$ or $p = 2.5$ and varying σ_q parameter in the range $\sigma_q \in < 0.1, 10 >$. It has already been noticed in Figs. 1 and 2 that the p RMSE and σ_q RMSE values are comparable for $\sigma_q = 0.5$ or $\sigma_q = 5$ for the same value of p. This can also be seen in Figs. 5 and 6, where for a variable σ_q value in the range $< 0.1, 10 >$ the p RMSE and σ_q RMSE values are kept at an average constant level.

Therefore, the p RMSE and σ_q RMSE values are more influenced by p than by σ_q for the considered values.

VII. CONCLUSION

GGD and augmented quaternions have been used in many engineering applications. In the literature you can find GGDs for different types of random variables. This allows you to model different processes and test different systems. The currently known GGDs with an augmented quaternion random variable are based on 3D GGD. That is, they are based on random variables with three components. The paper uses 4D GGD with four random components to correspond to the four components of a full quaternion. Based on this distribution, the probability density function for GGD with the an augmented quaternion random variable has been given. Then the definition of ℍ-properness was recalled and this QGGD has been simplified to GGD for an ℍ-proper quaternion random variable. For the latter distribution, the estimators have been derived using the ML method. In the experimental part, the performance of the estimators has been checked. It was shown that for the RMSE criterion a relatively large random sample is recommended.

REFERENCES

[1] G. Box and G. C. Tiao, *Bayesian Inference in Statistical Analysis*. Reading, MA, USA: Addison Wesley, 1973.

[2] R. J. Clarke, *Transform Coding of Images*. New York, NY, USA: Academic, 1985.

[3] Y. Du, "Ein sphärisch invariantes Verbunddichtemodell für Bildsignale," *Archiv Für Elektronik und Übertragungstechnik*, vol. 45, no. 3, pp. 148–159, May 1991.

[4] F. W. J. Olver, *Asymptotics and Special Functions*. New York, NY, USA: Academic, 1974.

[5] R. Krupiński, "Approximated fast estimator for the shape parameter of generalized Gaussian distribution for a small sample size," *Bull. Polish Acad. Sci. Tech. Sci.*, vol. 63, no. 2, pp. 405–411, Jun. 2015.

[6] F. Chapeau-Blondeau and A. Monir, "Numerical evaluation of the Lambert W function and application to generation of generalized Gaussian noise with exponent 1/2," *IEEE Trans. Signal Process.*, vol. 50, no. 9, pp. 2160–2165, Sep. 2002.

[7] R. Krupiński, "Reconstructed quantized coefficients modeled with generalized Gaussian distribution with exponent 1/3," *Image Process. Commun.*, vol. 21, no. 4, pp. 5–12, Dec. 2016.

[8] R. Krupiński, *Modeling Quantized Coefficients With Generalized Gaussian Distribution With Exponent* $1/m,\ m = 2, 3, \ldots$ (Advances in Intelligent Systems and Computing), vol. 659. Cham, Switzerland: Springer, 2018, pp. 228–237.

[9] C. Wang, "Research of image segmentation algorithm based on wavelet transform," in *Proc. IEEE Int. Conf. Comput. Commun. (ICCC)*, Oct. 2015, pp. 156–160.

[10] L. Ma, X. Wang, Q. Liu, and K. N. Ngan, "Reorganized DCT-based image representation for reduced reference stereoscopic image quality assessment," *Neurocomputing*, vol. 215, pp. 21–31, Nov. 2016. [Online]. Available: http://www.sciencedirect.com/science/article/pii/S0925231216306397

[11] C. Song, F. Li, Y. Dang, H. Gao, Z. Yan, and W. Zuo, "Structured detail enhancement for cross-modality face synthesis," *Neurocomputing*, vol. 212, pp. 107–120, Nov. 2016. [Online]. Available: http://www.sciencedirect.com/science/article/pii/S0925231216307007

[12] R. Krupiński, P. Lech, M. Tecław, and K. Okarma, "Binarization of degraded document images with generalized Gaussian distribution," in *Computational Science—ICCS 2019* (Lecture Notes in Computer Science), vol. 11540, J. M. F. Rodrigues, P. J. S. Cardoso, J. Monteiro, R. Lam, V. V. Krzhizhanovskaya, M. H. Lees, J. J. Dongarra, and P. M. Sloot, Eds. Cham, Switzerland: Springer, 2019, pp. 177–190.

[13] R. Krupiński and P. Mazurek, "Discrete Laplace estimator with a variable moment order for the modified image reconstruction," in *Proc. ICSES Int. Conf. Signals Electron. Circuits*, Sep. 2010, pp. 143–146. [Online]. Available: https://ieeexplore.ieee.org/document/5595230

[14] R. Krupiński and J. Purczyński, "Modeling the distribution of DCT coefficients for JPEG reconstruction," *Signal Process., Image Commun.*, vol. 22, no. 5, pp. 439–447, Jun. 2007. [Online]. Available: http://www.sciencedirect.com/science/article/pii/S0923596507000331

[15] R. Krupiński, "Recursive polynomial weighted median filtering," *Signal Process.*, vol. 90, no. 11, pp. 3004–3013, Nov. 2010. [Online]. Available: http://www.sciencedirect.com/science/article/pii/S0165168410001878

[16] R. Krupiński and E. Kornatowski, "The use of generalized Gaussian distribution in vibroacoustic detection of power transformer core damage," *Energies*, vol. 13, no. 10, p. 2525, May 2020. [Online]. Available: https://www.mdpi.com/1996-1073/13/10/2525

[17] E. Soave, G. D'Elia, and G. Dalpiaz, "Prognostics of rotating machines through generalized Gaussian hidden Markov models," *Mech. Syst. Signal Process.*, vol. 185, Feb. 2023, Art. no. 109767. [Online]. Available: https://www.sciencedirect.com/science/article/pii/S0888327022008354

[18] X.-Y. Wang, X. Shen, J.-L. Tian, P.-P. Niu, and H.-Y. Yang, "Statistical image watermark decoder using high-order difference coefficients and bounded generalized Gaussian mixtures-based HMT," *Signal Process.*, vol. 192, Mar. 2022, Art. no. 108371. [Online]. Available: https://www.sciencedirect.com/science/article/pii/S0165168421004084

[19] T. M. Nguyen, Q. M. J. Wu, and H. Zhang, "Bounded generalized Gaussian mixture model," *Pattern Recognit.*, vol. 47, no. 9, pp. 3132–3142, Sep. 2014. [Online]. Available: https://www.sciencedirect.com/science/article/pii/S0031320314001289

[20] J. Liu, "An image watermarking algorithm based on energy scheme in the wavelet transform domain," in *Proc. IEEE 3rd Int. Conf. Image, Vis. Comput. (ICIVC)*, Jun. 2018, pp. 668–672.

[21] M. N. Do and M. Vetterli, "Wavelet-based texture retrieval using generalized Gaussian density and Kullback–Leibler distance," *IEEE Trans. Image Process.*, vol. 11, no. 2, pp. 146–158, Feb. 2002.

[22] S. K. Choy and C. S. Tong, "Statistical wavelet subband characterization based on generalized gamma density and its application in texture retrieval," *IEEE Trans. Image Process.*, vol. 19, no. 2, pp. 281–289, Feb. 2010.

[23] S. Kasaei, M. Deriche, and B. Boashash, "A novel fingerprint image compression technique using wavelets packets and pyramid lattice vector quantization," *IEEE Trans. Image Process.*, vol. 11, no. 12, pp. 1365–1378, Dec. 2002.

[24] S. G. Chang, B. Yu, and M. Vetterli, "Adaptive wavelet thresholding for image denoising and compression," *IEEE Trans. Image Process.*, vol. 9, no. 9, pp. 1532–1546, Sep. 2000.

[25] S.-K. Choy and C.-S. Tong, "Supervised texture classification using characteristic generalized Gaussian density," *J. Math. Imag. Vis.*, vol. 29, no. 1, pp. 35–47, Oct. 2007.

[26] M. S. Allili, "Wavelet modeling using finite mixtures of generalized Gaussian distributions: Application to texture discrimination and retrieval," *IEEE Trans. Image Process.*, vol. 21, no. 4, pp. 1452–1464, Apr. 2012.

[27] P. Moulin and J. Liu, "Analysis of multiresolution image denoising schemes using generalized Gaussian and complexity priors," *IEEE Trans. Inf. Theory*, vol. 45, no. 3, pp. 909–919, Apr. 1999.

[28] G. Liu, J. Wu, and S. Zhou, "Probabilistic classifiers with a generalized Gaussian scale mixture prior," *Pattern Recognit.*, vol. 46, no. 1, pp. 332–345, Jan. 2013. [Online]. Available: https://www.sciencedirect.com/science/article/pii/S0031320312003329

[29] Y. Bazi, L. Bruzzone, and F. Melgani, "An unsupervised approach based on the generalized Gaussian model to automatic change detection in multitemporal SAR images," *IEEE Trans. Geosci. Remote Sens.*, vol. 43, no. 4, pp. 874–887, Apr. 2005.

[30] N. C. Beaulieu, H. Shao, and J. Fiorina, "P-order metric UWB receiver structures with superior performance," *IEEE Trans. Commun.*, vol. 56, no. 10, pp. 1666–1676, Oct. 2008.

[31] H. Abeida and J.-P. Delmas, "Slepian-bangs formulas for parameterized density generator of elliptically symmetric distributions," *Signal Process.*, vol. 205, Apr. 2023, Art. no. 108886. [Online]. Available: https://www.sciencedirect.com/science/article/pii/S016516842200425X

[32] K.-S. Song, "Globally convergent algorithms for estimating generalized gamma distributions in fast signal and image processing," *IEEE Trans. Image Process.*, vol. 17, no. 8, pp. 1233–1250, Aug. 2008.

[33] M. Novey, T. Adali, and A. Roy, "A complex generalized Gaussian distribution—Characterization, generation, and estimation," *IEEE Trans. Signal Process.*, vol. 58, no. 3, pp. 1427–1433, Mar. 2010.

[34] M. Novey, T. Adali, and A. Roy, "Circularity and gaussianity detection using the complex generalized Gaussian distribution," *IEEE Signal Process. Lett.*, vol. 16, no. 11, pp. 993–996, Nov. 2009.

[35] M. S. Greco, S. Fortunati, and F. Gini, "Naive, robust or fully-adaptive: An estimation problem for CES distributions," in *Proc. IEEE 8th Sensor Array Multichannel Signal Process. Workshop (SAM)*, Jun. 2014, pp. 457–460.

[36] E. Ollila, D. E. Tyler, V. Koivunen, and H. V. Poor, "Complex elliptically symmetric distributions: Survey, new results and applications," *IEEE Trans. Signal Process.*, vol. 60, no. 11, pp. 5597–5625, Nov. 2012.

[37] E. Ollila, J. Eriksson, and V. Koivunen, "Complex elliptically symmetric random variables—Generation, characterization, and circularity tests," *IEEE Trans. Signal Process.*, vol. 59, no. 1, pp. 58–69, Jan. 2011.

[38] P. A. Rodriguez, V. D. Calhoun, and T. Adalı, "De-noising, phase ambiguity correction and visualization techniques for complex-valued ICA of group fMRI data," *Pattern Recognit.*, vol. 45, no. 6, pp. 2050–2063, Jun. 2012. [Online]. Available: https://www.sciencedirect.com/science/article/pii/S0031320311002020

[39] A. Mehrabian, M. Sabbaghian, and H. Yanikomeroglu, "CNN-based detector for spectrum sensing with general noise models," *IEEE Trans. Wireless Commun.*, vol. 22, no. 2, pp. 1235–1249, Feb. 2023.

[40] E. Gómez, M. A. Gomez-Viilegas, and J. M. Marın, "A multivariate generalization of the power exponential family of distributions," *Commun. Statist. Theory Methods*, vol. 27, no. 3, pp. 589–600, Jan. 1998, doi: 10.1080/03610929808832115.

[41] J. K. Lindsey and P. J. Lindsey, "Multivariate distributions with correlation matrices for nonlinear repeated measurements," *Comput. Statist. Data Anal.*, vol. 50, no. 3, pp. 720–732, Feb. 2006. [Online]. Available: https://www.sciencedirect.com/science/article/pii/S0167947304002944

[42] F. Pascal, L. Bombrun, J.-Y. Tourneret, and Y. Berthoumieu, "Parameter estimation for multivariate generalized Gaussian distributions," *IEEE Trans. Signal Process.*, vol. 61, no. 23, pp. 5960–5971, Dec. 2013.

[43] Z. Boukouvalas, S. Said, L. Bombrun, Y. Berthoumieu, and T. Adali, "A new Riemannian averaged fixed-point algorithm for MGGD parameter estimation," *IEEE Signal Process. Lett.*, vol. 22, no. 12, pp. 2314–2318, Dec. 2015.

[44] N. Nacereddine, A. B. Goumeidane, and D. Ziou, "Unsupervised weld defect classification in radiographic images using multivariate generalized Gaussian mixture model with exact computation of mean and shape parameters," *Comput. Ind.*, vol. 108, pp. 132–149, Jun. 2019. [Online]. Available: https://www.sciencedirect.com/science/article/pii/S0166361518305967

[45] Y. Li, W. Cao, W. Hu, C. Gan, and M. Wu, "Fault detection for geological drilling processes using multivariate generalized Gaussian distribution and Kullback Leibler divergence," *IFAC-PapersOnLine*, vol. 53, no. 2, pp. 164–169, 2020. [Online]. Available: https://www.sciencedirect.com/science/article/pii/S2405896320303712

[46] Y. Li, W. Cao, W. Hu, Y. Xiong, and M. Wu, "Incipient fault detection for geological drilling processes using multivariate generalized Gaussian distributions and Kullback–Leibler divergence," *Control Eng. Pract.*, vol. 117, Dec. 2021, Art. no. 104937. [Online]. Available: https://www.sciencedirect.com/science/article/pii/S0967066121002148

[47] W. Hamilton, "On quaternions," *Proc. Royal Irish Acad.*, 1843.

[48] F. Zhang, "Quaternions and matrices of quaternions," *Linear Algebra Appl.*, vol. 251, pp. 21–57, Jan. 1997. [Online]. Available: http://www.sciencedirect.com/science/article/pii/0024379595005439

[49] P. O. Amblard and N. L. Bihan, "On properness of quaternion valued random variables," in *Proc. Int. Conf. Math. (IMA) Signal Process.*, 2004, pp. 23–26.

[50] N. Le Bihan, "The geometry of proper quaternion random variables," *Signal Process.*, vol. 138, pp. 106–116, Sep. 2017. [Online]. Available: https://www.sciencedirect.com/science/article/pii/S0165168417301093

[51] J. Vía, D. Ramírez, and I. Santamaría, "Properness and widely linear processing of quaternion random vectors," *IEEE Trans. Inf. Theory*, vol. 56, no. 7, pp. 3502–3515, Jul. 2010.

[52] C. Cheong Took and D. P. Mandic, "Augmented second-order statistics of quaternion random signals," *Signal Process.*, vol. 91, no. 2, pp. 214–224, Feb. 2011. [Online]. Available: http://www.sciencedirect.com/science/article/pii/S0165168410002719

[53] J. Navarro-Moreno, R. M. Fernández-Alcalá, and J. C. Ruiz-Molina, "A quaternion widely linear model for nonlinear Gaussian estimation," *IEEE Trans. Signal Process.*, vol. 62, no. 24, pp. 6414–6424, Dec. 2014.

[54] J. Vía, D. P. Palomar, L. Vielva, and I. Santamaría, "Quaternion ICA from second-order statistics," *IEEE Trans. Signal Process.*, vol. 59, no. 4, pp. 1586–1600, Apr. 2011.

[55] Y. Xia, M. Xiang, Z. Li, and D. P. Mandic, "Echo state networks for multidimensional data: Exploiting noncircularity and widely linear models," in *Adaptive Learning Methods for Nonlinear System Modeling*, D. Comminiello and J. C. Príncipe, Eds. Oxford, U.K.: Butterworth-Heinemann, 2018, pp. 267–288. https://www.sciencedirect.com/science/article/pii/B9780128129760000166

[56] C. Cheong Took and D. P. Mandic, "A quaternion widely linear adaptive filter," *IEEE Trans. Signal Process.*, vol. 58, no. 8, pp. 4427–4431, Aug. 2010.

[57] J. Navarro-Moreno, R. M. Fernandez-Alcala, and J. C. Ruiz-Molina, "A quaternion widely linear series expansion and its applications," *IEEE Signal Process. Lett.*, vol. 19, no. 12, pp. 868–871, Dec. 2012.

[58] C. Jahanchahi and D. P. Mandic, "A class of quaternion Kalman filters," *IEEE Trans. Neural Netw. Learn. Syst.*, vol. 25, no. 3, pp. 533–544, Mar. 2014.

[59] C. C. Took, G. Strbac, K. Aihara, and D. P. Mandic, "Quaternion-valued short-term joint forecasting of three-dimensional wind and atmospheric parameters," *Renew. Energy*, vol. 36, no. 6, pp. 1754–1760, Jun. 2011. [Online]. Available: https://www.sciencedirect.com/science/article/pii/S0960148110005677

[60] M. Xiang, B. S. Dees, and D. P. Mandic, "Multiple-model adaptive estimation for 3-D and 4-D signals: A widely linear quaternion approach," *IEEE Trans. Neural Netw. Learn. Syst.*, vol. 30, no. 1, pp. 72–84, Jan. 2019.

[61] H. Zhang and H. Lv, "Augmented quaternion extreme learning machine," *IEEE Access*, vol. 7, pp. 90842–90850, 2019.

[62] S. Zhu, H. Wang, H. Lv, and H. Zhang, "Augmented online sequential quaternion extreme learning machine," *Neural Process. Lett.*, vol. 53, no. 2, pp. 1161–1186, Apr. 2021, doi: 10.1007/s11063-021-10435-8.

[63] E. Grassucci, D. Comminiello, and A. Uncini, "An information-theoretic perspective on proper quaternion variational autoencoders," *Entropy*, vol. 23, no. 7, p. 856, Jul. 2021. [Online]. Available: https://www.mdpi.com/1099-4300/23/7/856

[64] Q. Li, "RUL estimation for rolling bearings using augmented quaternion-based least mean P-power with correntropy induced metric under framework of sparsity," *IEEE/ASME Trans. Mechatronics*, vol. 28, no. 2, pp. 976–989, Apr. 2023.

[65] Q. Li and Z. Ren, "A new fractional-order augmented quaternion-valued approach for degradation prognostics of bearings using generalized Hamilton-real calculus," *IEEE Trans. Instrum. Meas.*, vol. 71, pp. 1–11, 2022.

[66] A. Oya, "RKHS representations for augmented quaternion random signals: Application to detection problems," *Mathematics*, vol. 10, no. 23, p. 4432, Nov. 2022. [Online]. Available: https://www.mdpi.com/2227-7390/10/23/4432

[67] N. Le Bihan and P. Amblard, "Detection and estimation of Gaussian proper quaternion valued random processes," in *Proc. IMA Conf. Math.*, Jan. 2006, pp. 23–26.

[68] D. Venkatraman, V. V. Reddy, and A. W. H. Khong, "On the use of the quaternion generalized Gaussian distribution for footstep detection," in *Proc. IEEE Int. Conf. Acoust., Speech Signal Process.*, May 2013, pp. 6521–6525.

[69] R. Krupiński, "Generating augmented quaternion random variable with generalized Gaussian distribution," *IEEE Access*, vol. 6, pp. 34608–34615, 2018.

[70] R. Krupiński, "Generalized Gaussian distribution with augmented pure quaternion random variable," in *Proc. 27th Int. Conf. Methods Models Autom. Robot. (MMAR)*, Aug. 2023, pp. 45–50.

[71] G. Verdoolaege and P. Scheunders, "On the geometry of multivariate generalized Gaussian models," *J. Math. Imag. Vis.*, vol. 43, no. 3, pp. 180–193, Jul. 2012.

[72] L. Bombrun, F. Pascal, J.-Y. Tourneret, and Y. Berthoumieu, "Performance of the maximum likelihood estimators for the parameters of multivariate generalized Gaussian distributions," in *Proc. IEEE Int. Conf. Acoust., Speech Signal Process. (ICASSP)*, Mar. 2012, pp. 3525–3528.

ROBERT KRUPIŃSKI received the B.S. and M.S. degrees in computer engineering and the Ph.D. degree in technical sciences from Szczecin University of Technology, Szczecin, Poland, in 2002 and 2006, respectively.

From 2006 to 2009, he was an Assistant Professor with the Department of Signal Processing and Multimedia Engineering, Szczecin University of Technology. Since 2009, he has been an Assistant Professor with the Department of Signal Processing and Multimedia Engineering, West Pomeranian University of Technology in Szczecin. After graduation, he was with the IT industry. His research interests include signal and image processing and software engineering.

TOMASZ MARCINIAK received the Ph.D. degree in telecommunication engineering from the University of Agriculture and Technology, Bydgoszcz, Poland, in 2005.

Since 2006, he has been with the Faculty of Telecommunications, Computer Science and Electrical Engineering, Bydgoszcz University of Science and Technology, Bydgoszcz, where he is currently a Professor PBS. His current research interests include wireless communications with specific interests in 5G and beyond 5G technologies, and signal processing techniques for wireless communication systems and network optimization.

OLUTAYO O. OYERINDE (Senior Member, IEEE) received the Ph.D. degree in electronic engineering from the University of KwaZulu-Natal, Durban, South Africa, in 2011.

Since 2013, he has been with the School of Electrical and Information Engineering, University of the Witwatersrand at Johannesburg, South Africa, where he is currently an Associate Professor. He is also a National Research Foundation (NRF) C2 Rated Scientist, a Registered Professional Engineer (Pr.Eng.) with the Engineering Council of South Africa (ECSA), a Registered Engineer (R.Eng.) with COREN, and a Corporate Member of NSE. His current research interests include wireless communications with specific interests in 5G and beyond 5G technologies and signal processing techniques for wireless communication systems. He is an Associate Editor of IEEE Access and an Editorial Board Member of the *International Journal of Sensors, Wireless Communications and Control*.